Int. J. Electrochem. Sci., 13 **(2018)** 6169 – 6189, doi: 10.20964/2018.07.11

International Journal of
ELECTROCHEMICAL
SCIENCE
www.electrochemsci.org

Biomass of Microalgae *Spirulina Maxima* as a Corrosion Inhibitor for 1020 Carbon Steel in Acidic Solution.

Larissa Soares Rodrigues, Anita Ferreira do Valle, Eliane D'Elia[*]

Instituto de Química, UFRJ, Avenida Athos da Silveira Ramos 149, Centro de Tecnologia, Bloco A, CEP 21941-909, Cidade Universitária, Rio de Janeiro, RJ, Brazil. Phone: +55 21 39387816
[*]E-mail: eliane@iq.ufrj.br

Received: 2 March 2018 / *Accepted:* 19 April 2018 / *Published:* 5 June 2018

In this paper, the biomass of the microalgae Spirulina maxima, a cyanobacterium that synthesizes high levels of protein, was studied as a natural inhibitor of the corrosion of carbon steel in 1mol L^{-1} HCl by weight loss measurements, potentiodynamic polarization curves, electrochemical impedance measurements and surface analysis by scanning electron microscopy (SEM). The biomass of the microalgae Spirulina maxima acted as a good corrosion inhibitor reaching an inhibition efficiency of 96.4% after 72 h of immersion for an inhibitor concentration of 100 mg L^{-1}. The Ea increased with the addition of the inhibitor that characterizes the physical adsorption of the molecules present in the biomass of microalgae on the surface. This adsorption blocked the anodic and cathodic sites. The HMWF isolated from the total biomass showed an inhibition efficiency equal to the total biomass, which suggests that the macromolecules as proteins are probably responsible for the inhibitory action observed by the microalgae biomass.

Keywords: Acid Corrosion, Carbon Steel, Inhibitor, microalgae *Spirulina maxima.*

1. INTRODUCTION

Corrosion problems arise from the interaction of aqueous solutions and carbon steel in industrial processes such as pickling, where the metal alloy comes in contact with concentrated acids to remove incrustations in the system. Although several synthetic compounds are effective in protecting metals from corrosion, most of them are toxic to the environment and humans, in addition to high production costs. The toxicity may manifest during the synthesis of the compound and its application [1, 2]

The concern for the environment has today increased interest in developing more sustainable methods such as the study of corrosion inhibitors that cause less environmental impact. Natural

corrosion inhibitors are more cost-effective to develop, rich in nutrients, widely available and are renewable sources of materials. In addition, plant extracts are generally inexpensive and can be obtained by simple extraction procedures [1].

There are many studies that focus on the development of cost-effective and environmentally friendly compounds [1-12], some of which are dedicated to the use of algae as corrosion inhibitors for mild steel [13-17]. Microalgae are prokaryotic or eukaryotic microorganisms that perform aerobic photosynthesis. They have a wide range of natural compounds like pigments, lipids and fatty acids, proteins, polysaccharides, phenolic compounds, vitamins and others. They are used in various industries, such as pharmaceuticals, cosmetics, food industry, bioenergy applications, etc. [18-29].

Spirulina (Arthrospira) is a blue-green cyanobacterium with helical filaments. There are about 35 different spirulina strains, including S. maxima [20, 30]. This microalga is known for its exceptional amount of protein, 50-70% in its composition. Several studies suggest a composition between 5-7% of total lipids and 13-25% carbohydrates in the composition of these microalgae [19, 22]. The most salient acid among the various fatty acids present in its composition are palmitic acid and alpha-linolenic acid [22, 29]. It also contains more than 12 amino acids, vitamins (A, B1, B2, B6, B12, E) and minerals such as calcium, iron, magnesium, manganese, potassium, zinc, phosphorus and sodium. The pigments include phycocyanin, carotene and chlorophyll a [19, 22, 29, 31, 32].

The chemical composition of the algae biomass depends on its type and the environmental factors of the growth conditions to which the microalgae may be exposed during their cultivation. Factors such as temperature, illumination, salinity, amount of oxygen and minerals provide different amounts of natural compounds [20, 29, 33, 34, 35].

In this study, the microalgae Spirulina maxima were evaluated for their suitability as a natural corrosion inhibitor for 1020 carbon steel in 1 mol L^{-1} HCl by gravimetric tests, potentiodynamic polarization curves, electrochemical impedance measurements and surface analysis by scanning electron microscopy (SEM).

2. EXPERIMENTAL

2.1. Microalgal culturing

S. maxima was photoautotropically batch cultured in 9 L flasks containing 7 L of AO culture medium [36]. The cultures were fumigated with filtered atmospheric air using aquarial compressors with an air flow of 3.5 L min^{-1} and exposed to lateral illumination (120 μmol photons m^{-2} s^{-1} on the outer surface of the vessels) by fluorescent lamps (Philips 23W, white light) under a 12:12 h photoperiod. The culture flasks were maintained in an incubator (Forma Scientific Inc., Ohio, USA) at a temperature of 30±2 °C. The volume of culture medium was monitored and adjusted as necessary by adding sterile seawater to minimize the effects of evaporation. The cell growth was followed by optical density at 750 nm and to avoid the occurrence of a "lag phase" the cultures were adjusted to an initial optical density of 0.1 or 0.1 g L^{-1} dry weight.

2.2 Biomass composition

To analyze the biomass composition of Spirulina maxima, batch cultures were grown in 9 L glass carboys containing 7 L of AO culture medium [36], three independent biological replicates per species, according to the described microalgae cultivation. The biochemical composition was assayed in the exponential growth phase (seventh day) when the culture reached 1 g / l dry weight. The cells were centrifuged at 10,000 x g for 10 minutes at room temperature (Sorvall RC5B, Thermo Fisher Scientific). Thereafter, the biomass was dried at 37 ± 2 °C to constant weight. After weighing, the material was stored in desiccators until further biochemical analysis.

2.3 Biomass analytical methods

The samples for protein analysis were treated with 1 ml of distilled water for 24 hours at room temperature instead of 4 °C [37]. After the samples had been macerated and the total proteins quantitated in solution by the Lowry method, bovine serum albumin was used as the standard [38] modified by Mota [39]. The carbohydrate content was extracted in 80% H_2SO_4 according to the Myklestad and Haug methods [40]. The carbohydrate concentration was determined spectrophotometrically at 485 nm (Shimadzu, UV 1800 model) by the phenol-sulfuric acid method [41] using glucose as a standard. The total lipids were extracted by the Folch method [42] and quantified gravimetrically after solvent evaporation. The ash content was determined according to the Association of Analytical Communities-AOAC [43]. To do this, crucibles containing the samples were placed in a muffle furnace at 450 °C until a constant weight was achieved and then weighed.

2.4 Inhibitor preparation

During the 16 days of the cultivation period, the culture suspensions were continuously aerated with filtered air. After cultivation, the culture was centrifuged in the SORVALL, RC-5B centrifuge at 12000 rpm for approximately 15 minutes at 20 °C. The concentrated biomass was placed in petri dishes and dried at a temperature of about 37 °C. The dried biomass was conditioned in a desiccator until use.

The high molecular weight fractions (HMWF) and the low molecular weight fractions (LMWF) were separated from the liquid culture of Spirulina maxima using an ultrafiltration process where a specific ultrafiltration membrane (Millipore, EUA) with a molecular weight cut off point of 10 kDa was used. The fraction retained on the membrane are the high molecular weight fractions.

2.5 Specimen preparation

The chemical composition of 1020 carbon steel was (wt%): C: 0.18, P: 0.04, S: 0.05, Mn: 0.30, and the remaining percentage of Fe.

For gravimetric tests, specimens of about 14 cm^2 were abraded with 100 grade sandpaper, sandblasted, washed with double distilled water, degreased with acetone and air dried.

For the electrochemical experiments, the working electrode with a surface area of approximately 0.785 cm^2 was used for the potentiodynamic polarization curves and electrochemical impedance spectroscopy (EIS) measurements. The exposed area was mechanically abraded with 100, 320, 600, 1200 and 2000 grade abrasive paper and then washed with double distilled water, degreased with acetone and finally dried before each test.

2.6 Solution preparation

All tests were carried out using 1 mol L^{-1} hydrochloric acid solution as electrolyte which was prepared using 37% hydrochloric acid, from Merck Co. (Darmstadt, Germany) and double distilled water.

2.7 Weight loss experiment

The tests were performed in the absence and presence of extracts containing 100, 200, 400 and 800 mg L^{-1} inhibitor in 1 mol L^{-1} HCl medium for 2 hours immersion time at room temperature. The different immersion time tests were carried out at intervals of 2, 4, 24, 48 and 72 hours in the absence and presence of 100 mg L^{-1} biomass of S. maxima.

The temperature variation tests were performed at 35, 45, 55 and 65 °C for 2 hours immersion time in the absence and presence of 100 mg L^{-1} of the inhibitor. The weight loss measurements were obtained according to ASTM G31-7 using an analytical balance with an accuracy of 0.1 mg.

The inhibition efficiency (*IE*%) was obtained using the following equation:

$$IE\% = \frac{W_0 - W}{W_0} \times 100 \qquad (1)$$

Where, W_0 is the corrosion rate (g cm^{-2} h^{-1}) in the absence of the inhibitor and W is the corrosion rate in the presence of the inhibitor.

The apparent activation energy for the dissolution of the carbon steel in 1mol L^{-1} HCl was determined graphically from the Arrhenius equation (Eq. 2).

$$\log W = \frac{-E_a}{2.303RT} + \log A \qquad (2)$$

Where W is the corrosion rate (g cm^{-2} h^{-1}), E_a is the activation energy (kJ mol^{-1}), A is the pre-exponential factor, T is the absolute temperature (K) and R is the constant of ideal gases (8.314 J K^{-1} mol^{-1}).

In this study, each experiment was repeated under the same conditions three times, where the corrosion rate was obtained by averaging the results from the three tests.

2.8 Electrochemical methods

Electrochemical measurements were performed in a three-electrode glass cell: carbon steel as working electrode, saturated calomel electrode (SCE) as reference and a platinum wire with a large surface area as a counter electrode.

The electrochemical experiments were performed using an Autolab PGSTAT 128 N potentiostat/galvanostat, controlled by GPES 4.9 electrochemical software from Metrohm Autolab (The Netherlands).

Before each measurement, the open-circuit potential (OCP) was recorded as a function of time for 4000 seconds. The electrochemical impedance measurements were carried out using a frequency range of 100 kHz to 10 mHz at the stable open-circuit potential with an AC wave of 10 mV (rms). Potentiodynamic anodic and cathodic polarization curves were performed using a scan rate equal to 1 mV s^{-1} from –300 mV up to +300 mV in relation to the stable open-circuit corrosion potential.

The impedance and polarization parameters such as double layer capacitance (C_{dl}), charger transfer resistance (R_{ct}), corrosion current (j_{corr}), corrosion potential (E_{corr}), anodic Tafel slope (β_a) and cathodic Tafel slope (β_c) were computed from the polarization curves and Nyquist plots.

The inhibition efficiency (*IE%*) was calculated from potentiodynamic polarization curves and electrochemical impedance diagrams as follows:

$$IE\% = \frac{j_{corr,0} - j_{corr}}{j_{corr,0}} \times 100 \quad (3)$$

Where $j_{corr,0}$ is the corrosion current density in the absence of the inhibitor and j_{corr} is the corrosion current density in the presence of the inhibitor obtained from the Tafel plots.

$$IE\% = \frac{R_{ct} - R_{ct,0}}{R_{ct}} \times 100 \quad (4)$$

Where $R_{ct,0}$ is the charge-transfer resistance in the absence of the inhibitor and R_{ct} is the charge-transfer resistance in the presence of the inhibitor obtained from the electrochemical impedance diagrams.

2.9 Surface analysis

The specimens used for the surface morphology examination were mechanically abraded with 100, 320, 600, 1200 and 2000 grade emery paper and immersed in 1 mol L^{-1} HCl in the absence and presence of 100 mg L^{-1} of the inhibitor at room temperature for 2 h. The analysis was performed using an FEI Quanta 400 scanning electron microscope with an accelerating voltage of 20 kV.

3. RESULTS AND DISCUSSION

3.1 Spirulina maxima characterization

The biochemical composition of the dry biomass of Spirulina maxima grown in AO culture medium was determined and these results were shown in Table 1. The algal biomass contained large

amounts of protein (66.7 ± 0.6%) compared to reported work [44, 45]. Although the lipid content (0.8 ± 0.3) was similar to these reports, carbohydrates and ash content were different. These differences may be related to the species used, the methods of analysis and the culture systems of the microalgae. The high ash content (34.0%) found in this work was also reported in the literature [47], in which the ash content of S. maxima biomass was 30.9%. The inorganic compounds found in the biomass of S. maxima are related to the minerals Fe (93.6 mg / kg) and Mn (24.6 mg / kg) [47].

Table 1. Biochemical composition of dry biomass of *Spirulina maxima* grown in AO culture medium at 30 ± 2 ˚C and 120 μmol photons m^{-2} s^{-1}.

Time (day)	Protein (%)	Carbohydrate (%)	Lipid (%)	Ash (%)
7	66.7 ± 0.6	1.6 ± 0.05	0.8 ± 0.3	34.0 ± 2.6

3.2 Weight loss measurements

3.2.1 Tests varying inhibitor concentration and immersion time

Table 2. Immersion gravimetric assays for carbon steel in 1 mol L^{-1} HCl solution in the presence and absence of extracts from *Spirulina maxima* biomass.

Time (h)	**[Inhibitor]** (mg L^{-1})	***W*** (g cm^{-2} h^{-1})	***SD*** (g cm^{-2} h^{-1})	***IE%***
2	0	$3.30x10^{-3}$	$5.60x10^{-5}$	-
2	100	$1.26x10^{-3}$	$7.50x10^{-5}$	61.8
2	200	$1.03x10^{-3}$	$2.70x10^{-5}$	68.5
2	400	$9.65x10^{-4}$	$8.00x10^{-6}$	70.8
2	800	$9.05x10^{-4}$	$6.00x10^{-6}$	72.6
Time (h)		***W*** (g cm^{-2} h^{-1})	***SD*** (g cm^{-2} h^{-1})	***IE%***
2	-	$3.38x10^{-3}$	$1.30x10^{-4}$	-
	100 mg L^{-1} *S. maxima*	$1.16x10^{-3}$	$2.50x10^{-5}$	65.7
4	-	$4.50x10^{-3}$	$2.50x10^{-4}$	-
	100 mg L^{-1} *S. maxima*	$8.40x10^{-4}$	$1.00x10^{-6}$	82.3
24	-	$6.80x10^{-3}$	$1.00x10^{-4}$	-
	100 mg L^{-1} *S. maxima*	$1.18x10^{-3}$	$3.10x10^{-5}$	82.6
48	-	$1.27x10^{-2}$	$8.70x10^{-5}$	-
	100 mg L^{-1} *S. maxima*	$1.71x10^{-3}$	$5.50x10^{-5}$	86.5
72	-	$6.02x10^{-2}$	$6.52x10^{-3}$	-
	100 mg L^{-1} *S. maxima*	$2.14x10^{-3}$	$5.10x10^{-5}$	96.4

SD - standard deviation

The results of the weight loss measurements for carbon steel in 1 mol L^{-1} at different microalgae biomass concentrations and immersion times are shown in Table 2. The corrosion rate decreased with the addition of the inhibitor and the inhibition efficiency (*IE*%) increased with the concentration of the inhibitor due to the increase of the adsorbed constituent molecules of *Spirulina maxima* biomass on the metal surface, in higher concentrations, resulting in an increase in the surface coverage. The immersion time experiments were performed in the presence of 100 mg L^{-1} of the inhibitor. It's possible to observe an increase of the inhibition efficiency in longer immersion time, up to 96% of efficiency after 72 hours. The increase in *IE%* over time reveals the stability of the molecules of the biomass of microalgae *Spirulina maxima* on the metallic surface. In addition, these results indicate that the presence of molecules in the biomass has a long adsorption of carbon steel.

3.2.2 Effect of temperature

The temperature effect on the corrosion of 1020 carbon steel in 1 mol L^{-1} HCl solution was analyzed in the presence and absence of 100 mg L^{-1} of the *Spirulina maxima* biomass for two hours of immersion from 35 to 65 °C. The results are shown in Table 3.

Table 3. Temperature effect after two-hour immersion of carbon steel 1020 in aqueous solution of 1 mol L^{-1} HCl in the absence and presence of 100 mg L^{-1} of *Spirulina maxima biomass*.

Temperature (°C)		***W*** (g cm^{-2} h^{-1})	***SD*** (g cm^{-2} h^{-1})	***IE%***
35	-	$5.52x10^{-3}$	$3.10x10^{-4}$	-
	S maxima	$7.98x10^{-4}$	$6.00x10^{-5}$	85.5
45	-	$9.02x10^{-3}$	$4.20x10^{-5}$	-
	S. maxima	$1.72x10^{-3}$	$1.17x10^{-4}$	80.9
55	-	$1.40x10^{-2}$	$2.06x10^{-4}$	-
	S. maxima	$3.39x10^{-3}$	$1.31x10^{-4}$	75.8
65	-	$1.94x10^{-2}$	$3.59x10^{-4}$	-
	S. maxima	$6.29x10^{-3}$	$2.10x10^{-5}$	67.6

SD - Standard Deviation

The corrosion rate increases both in the absence and presence of an inhibitor as the temperature increases, the greater increase being in the presence of the inhibitor. Therefore, the efficacy of the inhibition decreased as the temperature increased, ranging from 85.5% to 67.6%. These results show that as the temperature of the solution increases, the desorption of the inhibitor molecules from the metal surface is most favored, resulting in a decrease in the coverage of the surface.

The Arrhenius plots for 1020 carbon steel in HCl solution in the absence and presence of the microalgae biomass are shown in Figure 1. The activation parameters (E_a, ΔH^* and ΔS^*) were

determined by the Arrhenius equation (Eq. 2) and by an alternative relation of the Arrhenius equation (Eq. 5):

$$W = RT/Nh \exp(\Delta S^*/R) \exp(-\Delta H^*/RT) \quad (5)$$

Where h is the Planck constant (6.63 x 10^{-34} J s), N is the Avogadro number (6.02 x 10^{23}), ΔS^* is the activation entropy and ΔH^* is the activation enthalpy.

The plot ln(W/T) vs. $1/T$ produces a line with an angular coefficient equal to $-\Delta H^*/R$ and a linear coefficient of ln(R/Nh) + $\Delta S^*/R$ (Figure 1B), from which ΔS^* and ΔH^* are calculated.

Table 4 shows the values of the activation functions (E_a, ΔH^* and ΔS^*) for the corrosion process of 1020 carbon steel in 1 mol L^{-1} HCl in the absence and presence of the microalgae biomass. From the data, it is possible to notice higher E_a e ΔH^* values in the presence of the inhibitor.

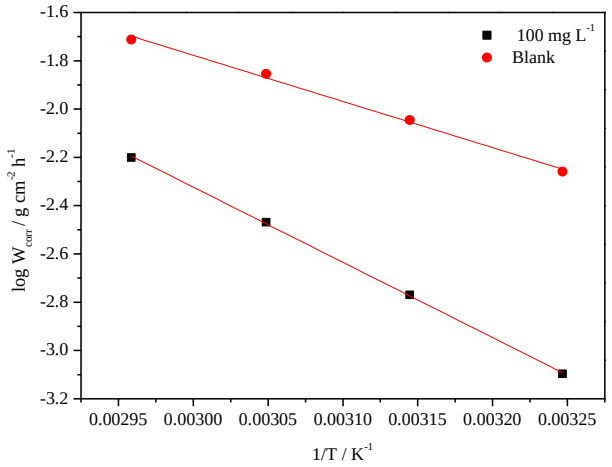

(A)

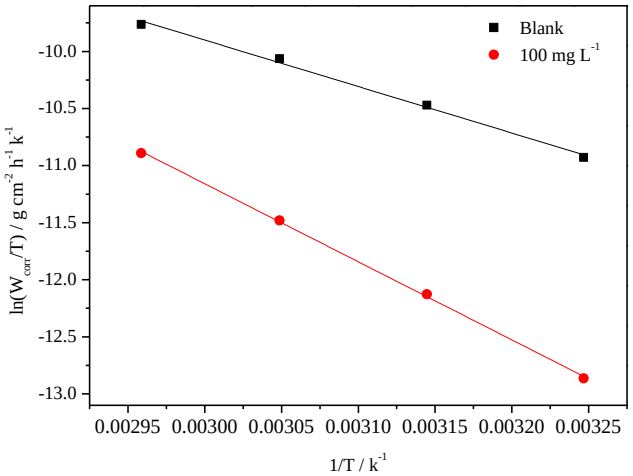

(B)

Figure 1. Arrhenius plots: (A) log$W$ *vs.* 1/T; (B) log (W/T) *vs.* $1/T$ for the corrosion of 1020 carbon steel, in the absence and presence of 100 mg L^{-1} of the *Spirulina maxima* biomass.

This result could be interpreted as due to a physical adsorption of the molecules present in the microalgae biomass on the metal surface. This conclusion is corroborated by the decrease in the inhibition efficiency with the increase in temperature.

Kamal and Sethuraman evaluated the influence of temperature on the corrosion of carbon steel by the inhibiting action of Spirulina platensis, and like S.maxima, S.platensis presented a physical adsorption of the constituents of microalgae on the metal surface [13] The authors attributed this physical adsorption to the fact that an increase in temperature caused the desorption of metal surface inhibitor components due to increased molecular agitation at higher temperatures versus weak interactions between the adsorbed molecules and the surface of metal.

The positive values of ΔH* reflect the endothermic nature of the process [11]. The values of Ea are higher than ΔH*, which indicates that the corrosion process must involve a gaseous reaction. In addition, the difference between Ea and ΔH* is 2.6 kJ mol^{-1}, which is equal to the average value of RT (2.6 kJ mol^{-1}) and indicates that the corrosion process is a unimolecular reaction. The negative values of ΔS* in the absence and presence of the extract indicate a step of association of the activated complex in the determinant step.

Table 4. Values of thermodynamic activation functions (E_a, ΔH^* and ΔS^*) for the corrosion process of carbon steel in 1 mol L^{-1} HCl in the absence and presence of the microalgae biomass.

	E_a (kJ mol^{-1})	ΔH^* (kJ mol^{-1})	ΔS^* (kJ K^{-1} mol^{-1})
Without *S. maxima*	36.5	33.9	-178
With *S. maxima*	59.5	56.9	-120

3.3. Electrochemical experiments

3.3.1. Open circuit potential

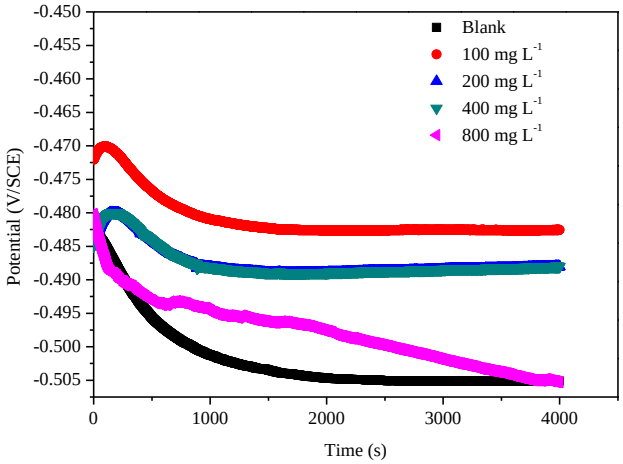

Figure 2. OCP plots of carbon steel samples in 1 mol L^{-1} HCl solution at different concentrations of the *S. maxima* biomass.

Prior to EIS measurements, OCP curves of 1020 carbon steel were recorded in the presence and absence of *S. maxima* biomass, as shown in Fig. 2.

Figure 2 shows that for the carbon steel in 1 mol L^{-1} HCl solution, the steady potential is reached after about 1500 s and the behavior is quite the same in the presence of 100, 200 and 400 mg L^{-1} microalgae biomass. In the presence of 800 mg L^{-1} inhibitor the OCP stabilization is longer, about 4000 s. The addition of the biomass of S. maxima slightly displaces the open circuit potential towards more positive values compared to the OCP in the blank solution, except in the presence of 800 mg of inhibitor of L^{-1}, whose value is the same as the blank solution..

3.3.2. Potentiodynamic polarization curves

Figure 3 presents the polarization curves for carbon steel 1020 in 1 mol L^{-1} HCl solution performed at concentrations 100, 200, 400 and 800 mg L^{-1} of *Spirulina maxima* biomass. The electrochemical parameters such as corrosion potential (E_{corr}), corrosion current density (j_{corr}), and the anodic (β_a) and cathodic (β_c) constants of Tafel, were obtained by the Tafel extrapolation method and are presented in Table 5.

It is observed that, as in the weight loss measurements, the inhibition efficiency increases with increasing inhibitor concentration, obtaining a maximum value of 93.9% for 800 mg L^{-1} of the *Spirulina maxima* biomass. Analyzing the results of Figure 3 it is possible to notice a decrease in the current density of both anodic and cathodic processes with the addition of the inhibitor, with the inhibition being more prominent in the cathodic branch.

Table 5. Electrochemical parameters obtained from anodic and cathodic polarization curves.

Concentration (mg L^{-1})	E_{OCP} (mV/SCE)	E_{corr} (mV/SCE)	β_a (mV dec^{-1})	$-\beta_c$ (mV dec^{-1})	j_{corr} (mA cm^{-2})	***IE%***
0	-505	-452	85.0	126	$5.77x10^{-1}$	-
100	-483	-455	78.0	102	$1.73x10^{-1}$	70.0
200	-492	-463	77.0	98	$1.54x10^{-1}$	73.3
400	-478	-466	79.0	112	$6.21x10^{-2}$	89.2
800	-505	-484	92.0	132	$3.54x10^{-2}$	93.9

In the cathodic domain, the values of β_c did not undergo significant changes after the addition of the microalgae biomass, which indicates that the addition of the inhibitor did not modify the mechanism of the reduction reaction of the hydrogen ions to H_2(g). The Tafel constant of the anodic branch (β_a) also did not undergo significant change with the addition of the inhibitor, which indicates that the inhibitor adsorbed on carbon steel probably does not alter the dissolution reaction of the metal

It was observed that the corrosion potential (E_{corr}), different from what was observed for OCP, moved little to more negative values after the addition of the inhibitor, which characterizes a more prominent inhibition of the cathodic reaction when the electrode is polarized. However, for an inhibitor to be considered anodic or cathodic it is necessary to have a potential difference of ± 85 mV in relation

to the potential of the blank [14]. From Table 5, it can be seen that the *OCP* and E_{corr} maximum displacement was +27 and −32 mV, respectively, indicating that *Spirulina maxima* biomass works as a mixed type inhibitor.

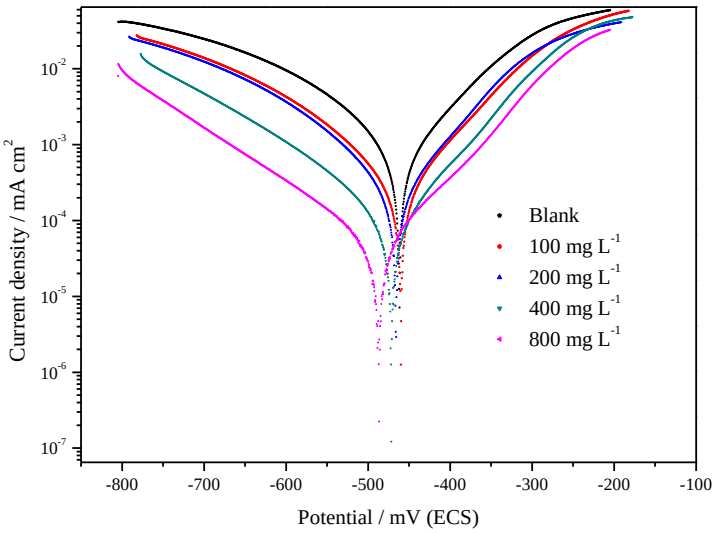

Figure 3. Anodic and cathodic polarization curves obtained for carbon steel in 1mol L^{-1} HCl solution at different concentrations of the microalgae biomass.

3.3.3. Electrochemical impedance spectroscopy (EIS)

Figure 4 and 5 present the Nyquist and Bode diagrams, respectively, for carbon steel in 1 mol L^{-1} HCl solution in the absence and presence of various concentrations of *Spirulina maxima* biomass.

The impedance diagrams obtained in the absence of the inhibitor (Fig. 4A) shows the presence of a single capacitive loop, attributed to the electric double layer capacitance and charge transfer resistance. It can be observed in Figure 4, a depressed capacitive loop, which is a characteristic of solid electrodes due to surface inhomogeneity during the corrosion process [3]. This behavior was not modified with the addition of the microalgae biomass indicating the activation-controlled nature of the reaction during a one-charge transfer process even in the presence of the inhibitor (Fig. 4B).

Figure 5 shows that the carbon steel immersed in 1mol L^{-1} HCl presents a single time constant. This behavior remains the same with the addition of the *S. maxima* biomass. The maximum phase angle in absence of the inhibitor is around 40° and in presence of microalgae biomass the maximum phase angle increases with the inhibitor concentration achieving around 70° at 800 mg L^{-1}. This increase in the maximum phase angle corroborates the adsorption of inhibitor molecules onto the metal surface.

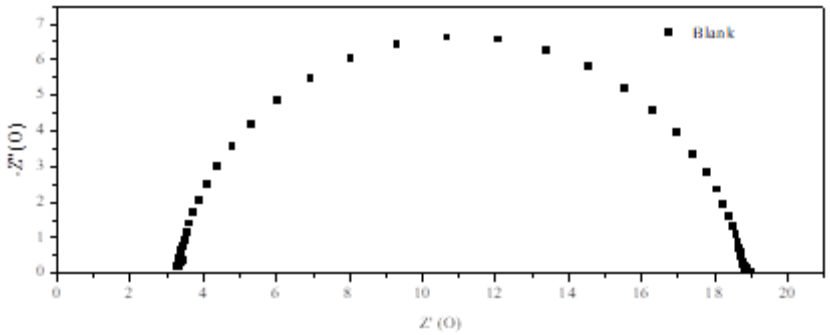

(A)

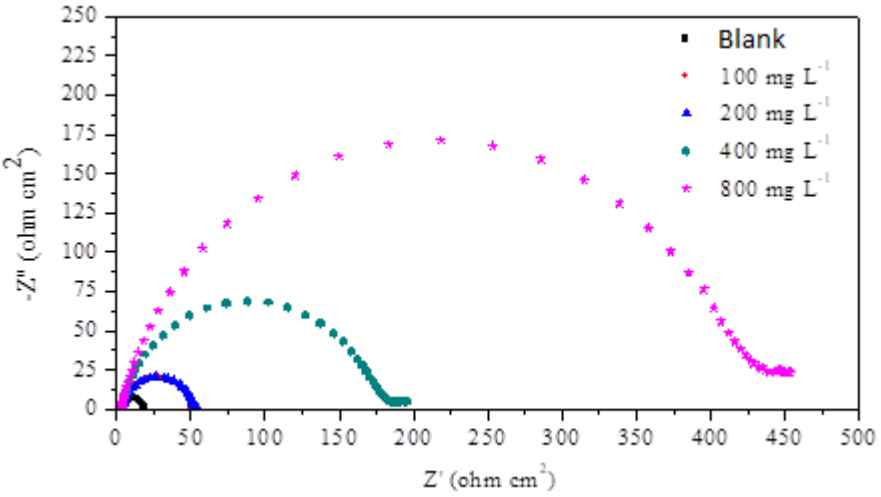

(B)

Figure 4. Nyquist plots obtained for 1020 carbon steel in 1 mol L^{-1} HCl solution in the absence (A) and presence of various concentrations of microalgae biomass (B).

The electrochemical impedance spectra obtained were analyzed using the equivalent circuit shown in figure 6, where R_s represents the ohmic resistance of the solution and R_{ct} is the resistance to the transfer of charge, whose value is inversely proportional to the corrosion rate. The constant phase element (*CPE*) was introduced into the circuit instead of the pure electric double layer capacitor in order to give more precision to the data adjustment. The *CPE* impedance is expressed by the following expression:

$$Z_{CPE} = Y_0^{-1}(j\omega)^{-n} \quad (6)$$

Where Y_0 is the *CPE* value, n is the *CPE* exponent and $j^2 = -1$.

The electric double layer capacitance (C_{dl}) for the circuit (Figure 6) was calculated from equation 7.

$$C_{dl} = Y_0 (\omega_{max})^{n-1} \quad (7)$$

Where $\omega_{max} = 2\pi f_{max}$, and f_{max} is the frequency when the imaginary component of the impedance is maximum [3].

Table 6 shows the electrochemical parameters of the impedance diagrams obtained for different concentrations of the inhibitor.

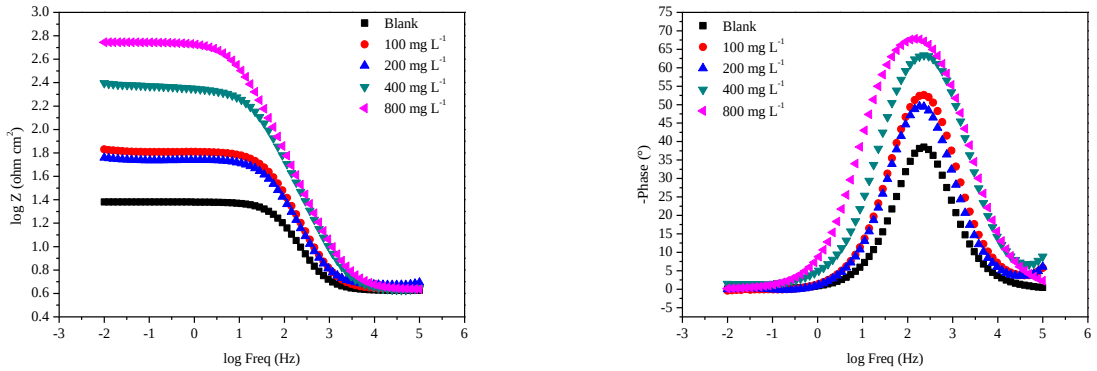

Figure 5. Bode plots for carbon steel in for 1020 carbon steel in 1 mol L^{-1} HCl solution in the absence and presence of various concentrations of microalgae biomass: (A) log|Z| *versus* log f and –Phase *versus* log f (B).

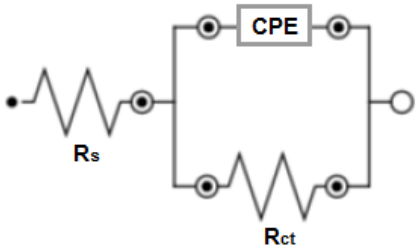

Figure 6. The equivalent circuit used to interpret the electrochemical impedance diagrams obtained for 1020 carbon steel in the absence and presence of the biomass.

Table 6. The electrochemical parameters obtained from the electrochemical impedance diagrams.

Concentration (mg L^{-1})	f_{max} (Hz)	R_{ct} (Ω cm^2)	Y_0 (μMho cm^{-2})	C_{dl} (μF cm^{-2})	n	***IE%***
0	90.5	19.8	181	94.8	0.898	-
100	44.9	60.6	107	56.9	0.888	67.3
200	44.9	61.6	108	59.7	0.895	67.9
400	22.3	228	67.5	33.8	0.860	91.3
800	8.80	552	58.4	33.3	0.860	96.4

The increase in the concentration of the inhibitor caused a decrease in the f_{max}, an increase in the charge transfer resistance (R_{ct}) and a decrease in the capacitance of the electric double layer, suggesting that the molecules present in the inhibitor act by the adsorption at the metal/solution interface, promoting surface blocking and making the charge transfer difficult. The inhibition efficiency reached 96.4% for microalgae biomass concentration of 800 mg L^{-1}.

3.4 Adsorption isotherm

The adsorption isotherms are important for understanding the interaction between the inhibitor molecules in the surface of carbon steel during the corrosion process. The experimental results were adjusted to different adsorption isotherms: Langmuir, Temkin and El-Awady, in order to study the adsorption behavior of *S. maxima* biomass constituents.

The inhibition efficiency is directly proportional to the adsorbed molecule fraction into the covered surface (θ), which was calculated using the R_{ct} values from the impedance diagrams, shown in Table 6.

$$\theta = IE\%/100 \quad (8)$$

Figure 7 displays the linear plots of the Langmuir (C/θ vs. C), Temkin (θ vs. logC) and El-Awady (log(θ/1-θ) vs. logC) isotherms.

According to the Bockris-Devanathan-Muller model, the solvent molecules are adsorbed in the metal/solution interface [$H_2O_{(ads)}$] and are exchanged by the molecules of the organic compounds present in the inhibitor [$Org_{(sol)}$] [3]:

$$Org_{(sol)} + xH_2O_{(ads)} \rightarrow Org_{(ads)} + xH_2O_{(sol)}$$

Where x is the replaced water molecules number by one organic inhibitor molecule.

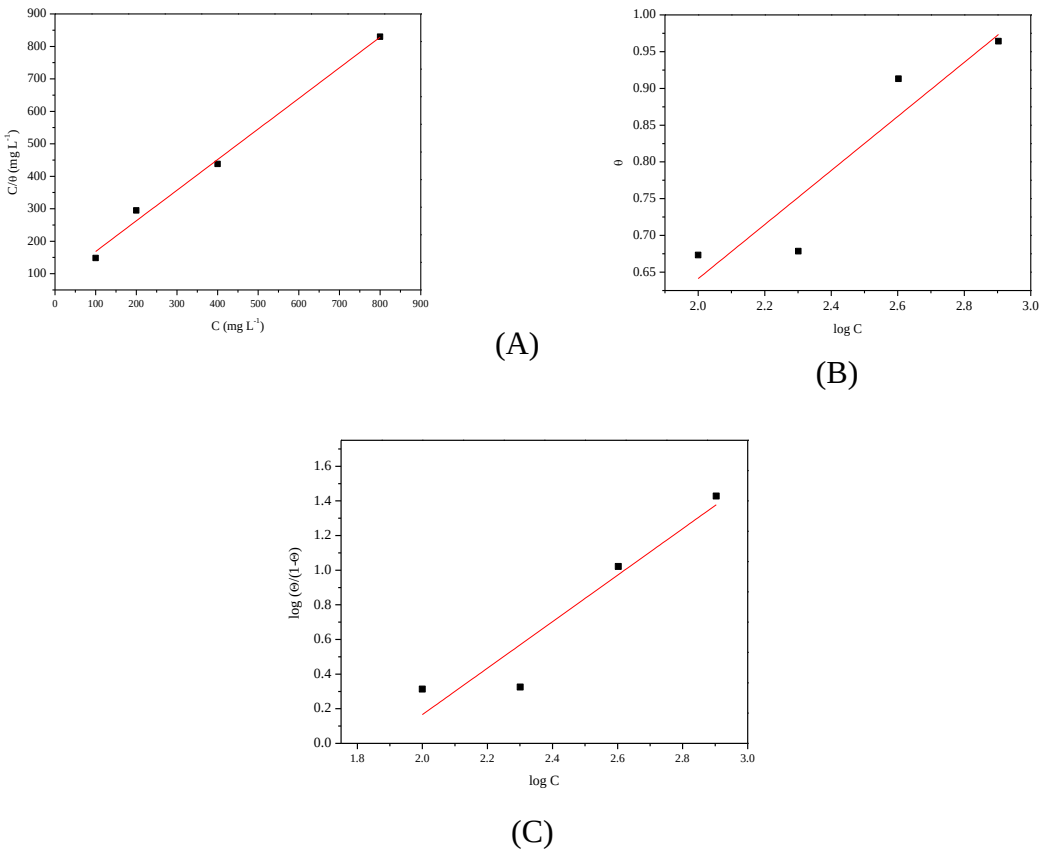

Figure 7. Langmuir (A), Temkin (B) and El-Awady (C) isotherms obtained from EIS data using *Spirulina maxima* extract as corrosion inhibitors.

Table 7. Data of straight lines obtained by linear adjustment

Isoterm	Line Equation	
Langmuir $C/\theta = 1/K_{ads} + C$	$y = 0.943\,x + 74.0$	0.994
Temkin $\theta = (-2{,}303/2a) \log K_{ads} + (-2{,}303/2a) \log C$	$y = 0.368\,x - 0.0944$	0.871
El-Awady $\log(\theta/(1-\theta)) = \log K_{ads} + y \log C$	$y = 1.34\,x - 2.52$	0.856

Langmuir isotherm assumes that the inhibition occurs by monolayer adsorption at the appropriate sites on the metal surface, which contains a fixed number of adsorption sites, and each site holds one adsorbate with no interaction between the adsorbed molecules.

El-Awady isotherm considers that an active site can be occupied by more than one molecule of the inhibitor or that a single inhibitor molecule can adsorb in more than one active site (parameter y). $y < 1$ show that a single molecule involved in the adsorption process has been adsorbed on more than one active site. Values of $1/y < 1$ suggest multilayer adsorption.

Temkin isotherm assumes that the heat of adsorption of all molecules that cover the adsorbent decreases linearly as a function of the coating due to the interaction between the adsorbed molecules. An attraction interaction is noticed when $a > 0$, and a repulsion interaction happens when $a < 0$ [3].

Table 7 shows the parameters for the different adsorption isotherms obtained for the *S. maxima* biomass as a corrosion inhibitor.

In studies on corrosion inhibitors, acceptable correlation coefficients fall generally between 0.99 and 0.60 [3]. For this study, all the isotherms presented acceptable linear correlation coefficients, but the Langmuir isotherm presents higher values, reaching 0.994. The Langmuir isotherm assumes that inhibitory molecules adsorb onto the surface without interactions between the adsorbed molecules and that the adsorption occurs at a specific and homogeneous site and each inhibitory molecule holds only one site [3, 7]. However, the angular coefficient obtained for the Langmuir isotherm was less than one (0.943), which indicates a deviation of the ideality, which could be explained by the existence of interactions between the adsorbed molecules and/or the number of inhibitory molecules occupying an active site is not the unit [3]. For the Temkin isotherm, the value of a is negative, suggesting a repulsive force between the adsorbed molecules [3]. The El-Awady isotherm shows a value of $1 / y < 1$, which suggests the adsorption of more than one molecule in the same active site with the formation of multiple layers between the inhibitor molecules and the metal surface. As the study with temperature variation proved that the adsorption is of a physical nature, the formation of multilayers is plausible.

3.5 Surface analysis

Figure 8 shows the surface analysis of 1020 carbon steel before the immersion (a), after immersion in 1 mol L^{-1} HCl for 2 h (b) and after immersion in 1 mol L^{-1} HCl containing 100 mg L^{-1} of *S. maxima* biomass for 2 h (c).

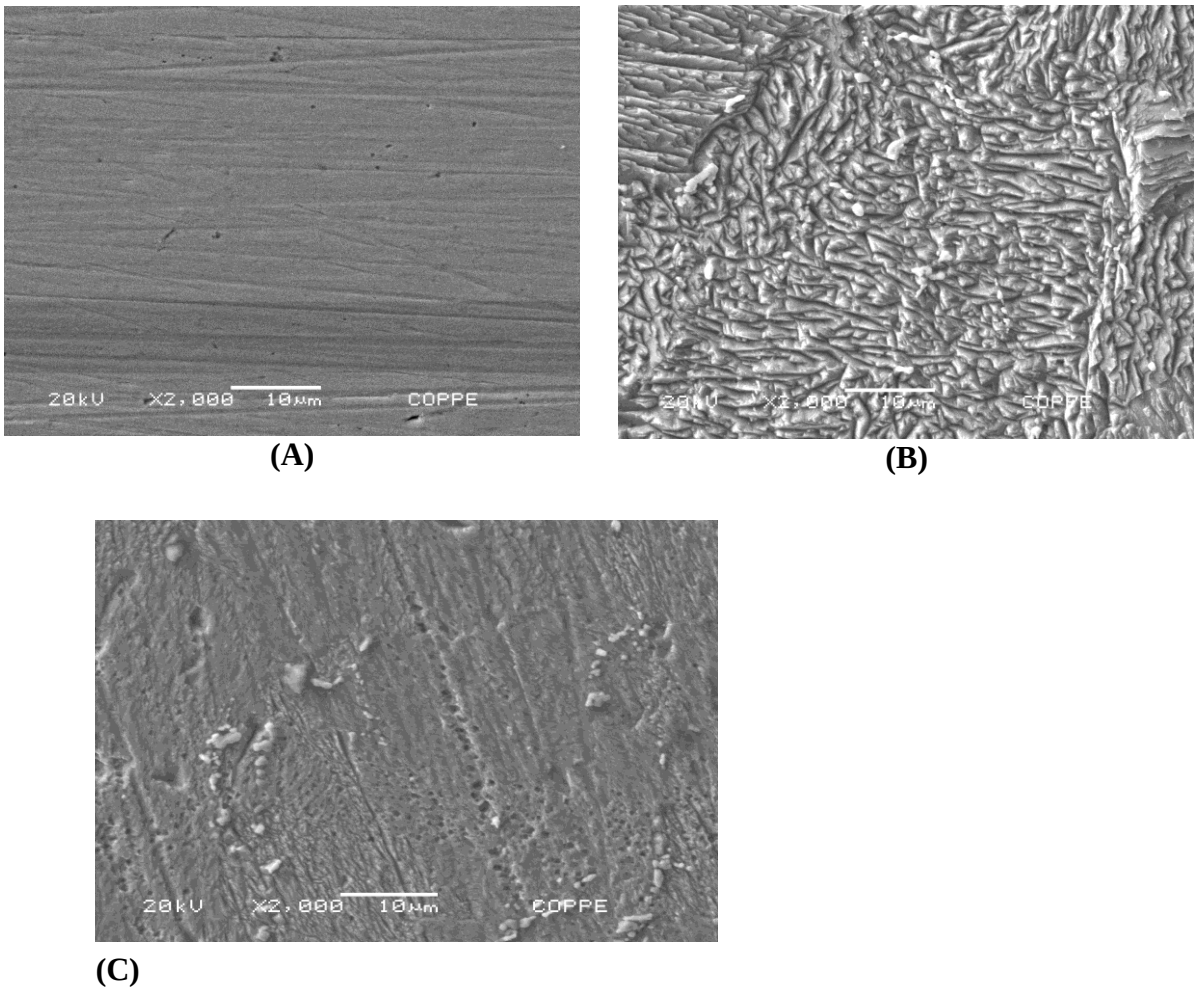

Figure 8. The surface analysis of the 1020 carbon steel using the SEM technique: (A) abraded surface before immersion; (B) immersed specimen for 2 hours in 1 mol L^{-1} HCl; (C) immersed specimen for 2 hours in 1 mol L^{-1} HCl in the presence of 100 mg L^{-1} *S. maxima* biomass. Magnitude: 2000x.

In the absence of the inhibitor (Fig. 8B), it is possible to observe a high roughness related to the attack of HCl on the surface of carbon steel 1020. In the presence of 100 mg of inhibitor of L^{-1} (figure 8C), the surface is much less rough and more uniform, being able to observe the polishing lines as those observed in (figure 8A). The analysis of the surface corroborates the weight loss and the electrochemical results, which shows that the microalgae S. maxima is effective in protecting the surface of carbon steel 1020 in HCl 1 mol L^{-1} medium.

3.6 Mechanism

S. maxima microalgae are known for their exceptional amount of protein, 50-70% in their composition. It also contains palmitic acid and alpha-linolenic acid, more than 12 amino acids, vitamins (A, B1, B2, B6, B12, E) and pigments such as phycocyanin, which is a pigment-protein complex and whose molecular weight is around 30,000 Da., Carotene and chlorophyll [19, 22, 29, 31, 32].

Based on this, the high molecular weight fraction (HMWF) was isolated from the microalgae biomass using a membrane with a molecular weight cutoff of 10 kDa. The low molecular weight fraction (LMWF) was also separated for the study. Both the HMWF and the LMWF were evaluated as corrosion inhibitors by potentiodynamic polarization curves and electrochemical impedance technique (the results are shown in Figures 9A and 9B, respectively).

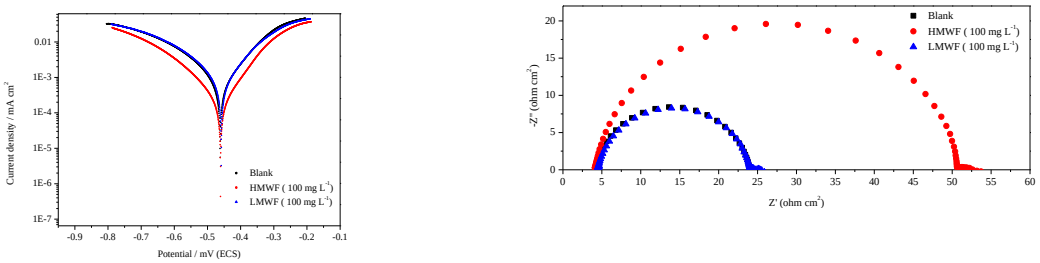

(A) (B)

Figure 9. The potentiodynamic polarization curves (A) and electrochemical impedance (B) for C-steel in 1 mol L^{-1} HCl in the absence and presence of 100 mg L^{-1} of HMWF and LMWF from *S. maxima* biomass.

Table 8. The electrochemical parameters obtained from the anodic and cathodic polarization curves of C-steel in 1 mol L^{-1} HCl in the absence and presence of HMWF and LMWF from *S. maxima* biomass.

Inhibitor (mg L^{-1})	OCP mV/SCE	E_{corr} mV/SCE	β_a mV dec^{-1}	$-\beta_c$ mV dec^{-1}	j_{corr} (mA cm^{-2})	*IE*%
0	-505	-452	85.0	126	$5.77x10^{-1}$	-
100	-483	-455	78.0	102	$1.73x10^{-1}$	70.0
HMWF	-488	-453	77.0	112	$1.89x10^{-1}$	67.2
LMWF	-491	-452	84.0	114	$5.59x10^{-1}$	3.11

Table 8 presents the kinetic parameters obtained from the anodic and cathodic curves in the presence of 100 mg L^{-1} HMWF and LMWF. It is possible to observe that the LMWF of the SM microalgae does not have an effective inhibiting effect on the corrosion of the carbon steel in 1 mol L^{-1} HCl medium.

Comparing the data of the polarization curves (Tables 8) for the biomass of S. maxima and its separated fractions (HMWF and LMWF), it is possible to say that the LMWF does not influence the corrosion inhibition, only the high molecular weight fraction which contains macromolecules as proteins are effective in the protection of 1020 carbon steel in acid medium.

Comparing 100 mg L^{-1} of the HMWF with the same concentration of the total microalgae biomass (Table 5), the IE almost did not change significantly, changing from 67% to 70%, However, the LMWF did not present a relevant inhibitory action, since its IE was extremely low due to its value of corrosion current density near the blank. The anodic and cathodic Tafel constants do not change

with the addition of HMWF and LMWF, which demonstrates that both do not change the mechanism of the reduction of hydrogen ions to H_2 (g) and the metallic dissolution reactions.

The impedance diagrams obtained in the presence of 100 mg L^{-1} HMWF and LMWF from S. maxima (figure 9B) show the presence of a single capacitive loop, attributed to the electric double layer capacitance and charge transfer resistance, the same behavior of the blank. However, an increase in the charge transfer resistance and a decrease in the capacitance of the electric double layer can be observed only for HMWF. Compared to the blank result, the LMWF does not change the diagram, resulting in 0.50% IE.

Therefore, low molecular weight molecules present in S. maxima biomass do not contribute to the corrosion inhibition of 1020 carbon steel, but high molecular weight molecules, such as proteins, present in large quantities in microalgae S Maximum seems to be responsible for the action of inhibition. The phytocyanin pigment, which is a pigment-protein complex, could also be responsible for the inhibition of corrosion.

Table 9. The electrochemical parameters obtained from the electrochemical impedance diagrams of C-steel in 1 mol L^{-1} HCl in the absence and presence of HMWF and LMWF from *S. maxima* biomass.

Inhibitor (mg L^{-1})	f_{max} (Hz)	R_{ct} (Ω cm^2)	Y_0 (μMho cm^{-2})	C_{dl} (μF cm^{-2})	n	***IE%***
0	90.5	19.8	181	94.8	0.898	-
100	44.9	60.6	107	56.9	0.888	67.3
HMWF	56.7	47.2	124	64.9	0.890	58.0
LMWF	71.6	19.9	240	119	0.885	0.50

The decrease in *IE* with temperature and increase of the activation energy for the tests in the presence of the inhibitor, evidenced a process of physical adsorption of the constituent molecules of *S. maxima* on the metallic surface. For the physical adsorption, it is possible to propose that the anions present (in this case, chloride ions) were first adsorb onto the metal surface making it negatively charged, and then the protonated inhibitory molecules (in this case, the acidic proteins) are electrostatically adsorbed on the carbon steel surface. This result could also explain the value of the negative a found in the fit of the data to the Tenkim isotherm, suggesting a repulsive force between the adsorbed molecules, i.e. between the protonated protein molecules.

Some works were dedicated to the use of algae as corrosion inhibitors for mild steel [13-15] in acidic media. Table 10 gives a comparison of the *IE%* of different algae. Good inhibition efficiencies can be achieved; however, *Spirulina maxima* biomass presented the highest IE reaching 96.4% for corrosion of carbon steel in HCl solution using 800 mg L^{-1} of microalga biomass. It is important to emphasize that for all algae the adsorption was physical type.

Table 10. Percentage of corrosion inhibition efficiency for some algae.

Alga	Concentration	Medium	Inhibition efficiency %	Nature adsorption	Ref
Spirulina platensis	500 mg L^{-1}	1 mol L^{-1} HCl 1 mol L^{-1} H_2SO_4	75.82 80.21	Physisorption	13
Hydroclathus chathratus	500 mg L^{-1}	1 mol L^{-1} HCl 1 mol L^{-1} H_2SO_4	65.28 77.64	Physisorption	14
Kappaphycus alvarezii	500 mg L^{-1}	1 mol L^{-1} HCl 1 mol L^{-1} H_2SO_4	69.33 77.41	Physisorption	15
Spirulina maxima	400 mg L^{-1} 800 mg L^{-1}	1 mol L^{-1} HCl	**91.3** **96.4**	Physisorption	**Present work**

4. CONCLUSIONS

- Both *Spirulina maxima* biomass and its high molecular weight fraction (HMWF) act as corrosion inhibitors of 1020 carbon steel in 1 mol L^{-1} HCl solution.

- The complex chemical composition of this microalga makes it difficult to associate the inhibitory action with only one constituent or constituents group, but it is possible to propose that the inhibition efficiency demonstrated by the weight loss and electrochemical results occur by the action of the protein molecules, since this compound is present in large amounts in *Spirulina maxima*, reaching 70% of the microalgae constituents.

- The temperature increase of the solution decreased inhibitory efficiency, suggesting physical adsorption of the compounds present in the biomass onto the metallic surface.

- The pigment such as phycocyanin, which is a pigment-protein complex, could be the responsible for the inhibitory action of the S. maxima biomass.

- The results of the potentiodynamic polarization and electrochemical impedance spectroscopy evidenced behavior that suggests the adsorption of the molecules present in the inhibitor at the metal / solution interface without changing the mechanism of the cathodic and anodic reactions.

- The presence of a less rough surface with the addition of the *S. maxima* biomass indicates that the extract of the *Spirulina maxima* microalgae is effective in protecting the surface of 1020 carbon steel in 1 mol L^{-1} HCl solution, thus confirming the results of the tests gravimetric and electrochemical tests.

ACKNOWLEDGEMENTS
This work was supported by CNPq (National Council for Scientific and Technological Development) [Grant Number 309353/ 2015-7, 153940/2015-8 and 424306/2016] and by FAPERJ (Foundation for Research Support of the State of Rio de Janeiro) [Grant Number E-26/010.001675/ 2014].

References

1. Singh, E.E. Ebenso and M.A. Quraishi, *Int. J. Corros.*, (2012) DOI: 10.1155/2012/897430
2. P.B. Raja and M. G. Sethuraman, *Mater. Lett.*, 62 (2008) 113.
3. V.V. Torres, G.B. Cabral, A.C.G. Silva, K.C.R. Ferreira and E. D'Elia, *Quím. Nova*, 39 (2016) 423.
4. B.E.A. Rani and B.B.J. Basu, *Int. J. Corros.*, (2012) DOI: 10.1155/2012/380217
5. J.C. Rocha, J.A.A.P. Gomes, E. D'Elia, A.P.C. Gil, L.M.C. Cabral, A.G. Torres and M.V.C. Monteiro, *Int. J. Electrochem. Sci*., 7 (2012) 11941.
6. J.C. Rocha, J.A.A.P. Gomes and E. D'Elia, *Mater. Res.*, 17 (2014) 1581.
7. J.C. Rocha, J.A.A.P. Gomes and E. D'Elia, *Corros. Sci.*, 52 (2010) 2341.
8. S. Paul and B. Kar, *ISRN Corrosion*, (2012) DOI: 10.5402/2012/641386.
9. G. Gunasekaran, S. Chongdar, S.N. Gaonkar and P.Kumar, *Corros. Sci.*, 46 (2004) 1953.
10. Y. Abboud , O. Tanane , A. El Bouari , R. Salghi , B. Hammouti , A. Chetouani and S. Jodeh, *Corros. Eng. Sci. Technol.*, 51 (2015) 557.
11. C.O. Akalezi, C.E. Ogukwe, E.A. Ejele and E.E. Oguzie, *Int. J. Corros.*, 5 (2016) 132.
12. N. Patni, S. Agarwal and P. Shah, *Chin. J. Eng.*, (2013) DOI: 10.1155/2013/784186.
13. C. Kamal and M.G. Sethuraman, *Arab. J. Chem.*, 5 (2013) 155.
14. C. Kamal and M.G. Sethuraman, *Res. Chem. Intermed.*, 39 (2013) 3713.
15. C. Kamal and M.G. Sethuramank, *Mater. Corros.*, 65 (2014) 846.
16. B.D Mert, M.E. Mert, G. Kardas and B. Yazici, *Mater. Chem. Phys.*, 130 (2011) 697.
17. M. Shi-De, Y. Xiao-Jin, F. Xiao, C. Yu-Min, F. Guo-Ming and D. Ai-Ling, *Chin. J. Oceanol. Limnol.*, 17 (1999) 375.
18. D.B Stengel, S. Connan and Z.A. Popper, *Biotechnol. Adv.*, 26 (2011) 483.
19. S.S Roy and R. Pal., *Proc. Zool. Soc*., 68 (2014) 1.
20. M. Koller, A. Muhr and G. Braunegg., *Algal Res.*, 6 (2014) 52.
21. G. Tang and P.M. Suter., *J. Pharm.Nutr. Sci.*, 1 (2011) 111.
22. J. Falquet, Ant. Tech., (2017) http://antenna.ch/en/documents/AspectNut_UK.pdf
23. S.M. Hoseini, K. Khosravi-Darani and M.R. Mozafari. *Rev. Med. Chem.*, 13 (2013) 1231.
24. L. brennaan and P. Owende., *Renew. Sust. Energ. Rev.*, 14 (2010) 557.
25. K.H.M. Cardozo, T. Guaratini, M.P. Barros, V.R. Falcão, A.P. Tonon, N.P Lopes, S. Campos, M.A. Torres, A.O. Souza, P. Colepicolo and E. Pinto., *Comp. Biochem. Physiol.*, 146 (2007) 60.
26. G. Chamorro, M. Salazar, L. Favila and H. Bourges, *Rev. Inv. Clín*. 48 (1996) 389.
27. T. Hirata, M. Tanaka, M. Ooike, T. Tsunomura and M. Sakaguchi, *J. Appl. Phycol.*, 12 (2000) 435.
28. H-L. Wu, G-H. Wang, W-Z. Xiang, T. Li and H. He, *Int. J. Food Prop.*, 19 (2016) 2349.
29. A.P. Batista, L. Gouveia, N.M. Bandarra, J.M. Franco and A. Raymundo, *Algal Res.*, 2 (2013) 164.
30. S-H. Oh, J. Ahn, D. Kang and H. Lee. *Mar. Biotechnol.*, 13 (2011) 205.
31. Z. Khan, P. Bhadouria and P.S. Bisen, *Curr. Pharm. Biotechnol.*, 6 (2005) 373.
32. L. Bennamoun, M. T Afzal and A. Léonard, *Renew. Sust. Energ. Rev.*, 50 (2015) 1203.
33. G.G. Salmean, L.F. Castillo and G.C. Cevallos, *Nutric. Hospit.*, 32 (2015) 34.
34. A. Ranga Rao, C. Dayananda, R. Sarada, T.R. Shamala and G.A. Ravishankar, *Bioresour. Technol.*, 98 (2007) 560.
35. A.M. Santos, P.P. Lamers and R.H. Wijffels, *Algal Res.*, 2 (2013) 204.
36. S. Aiba and T. Ogawa, *J. Gen. Microbiol.*, 102 (1977) 179.
37. E. Barbarino and S. O Lourenço, *J. Appl. Phycol.*, 17 (2005) 447.
38. O.H. Lowry, N. J. Rosebrough, A.L Farr and R. J. Randall, *J. Biol. Chem*., 193 (1951) 265.
39. M. Mota, Caracterização e hidrólise enzimática da microalga *Chlorella pyrenoidosa*. Universidade Federal do Rio de Janeiro, Rio de Janeiro, Brasil (2015).
40. S. Myklestad and A. Haug, *Exp. Mar. Biol. Ecol*., 9 (1972) 125.

41. M. Dubois, K. A. Gilles, J. K Hamilton, P. A Rebers and F. Smith, *Anal. Chem*. 28 (1956) 350.
42. J. Foch, M. Lees and G.H.S. Stanley, *J. Biol. Chem.*, 226 (1957) 497.
43. AOAC, Official methods of analysis, Association of Official Analytical Chemists, (1990) Virginia, United States of America.
44. K. Barros, Produção de biomassa de Arthrospira platensis (*Spirulina platensis*) para alimentação humana. Universidade Federal da Paraíba, Paraíba, Brasil (2010).
45. J. Carvajal, Caracterização e modificações químicas da proteína da microalga *Spirulina* (*Spirulina maxima*). Universidade Federal da Paraíba, Paraíba, Brasil (2009).